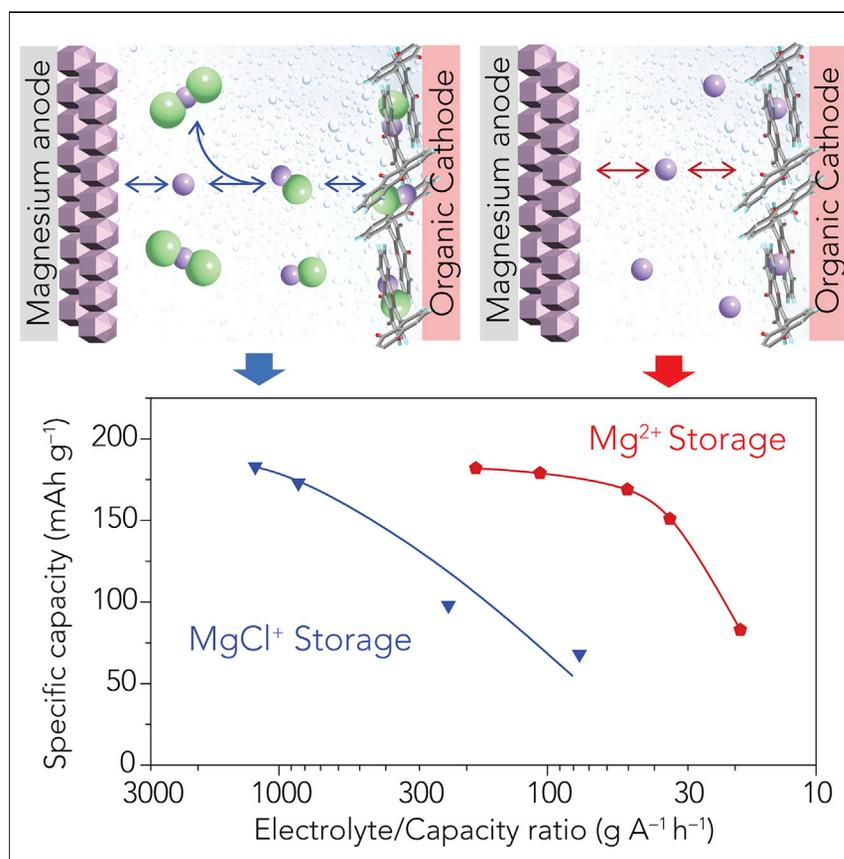


## Article

## Directing Mg-Storage Chemistry in Organic Polymers toward High-Energy Mg Batteries



In typical chloride-containing electrolytes, storage of MgCl<sup>+</sup> is dominant in organic cathodes. The negative impact of the MgCl-storage chemistry on the specific energy was elucidated through cell tests with controlled amounts of electrolyte. With the right combination of organic cathodes and chloride-free electrolytes, storage of Mg<sup>2+</sup> in organic electrodes can be realized. The Mg-storage chemistry has also enabled the first Mg battery that operates under lean electrolyte conditions, which has important implications for the practicality of high-energy organic Mg batteries.

Hui Dong, Yanliang Liang, Oscar Tutusaus, Rana Mohtadi, Ye Zhang, Fang Hao, Yan Yao

yliang7@central.uh.edu (Y.L.)  
yyao4@uh.edu (Y.Y.)

## HIGHLIGHTS

Storage of MgCl<sup>+</sup> is dominant in organic cathodes in chloride-containing electrolytes

First demonstration of authentic organic Mg-ion batteries with chloride-free electrolytes

Mg-storage chemistry enables the Mg battery to operate under lean electrolyte conditions

Polymers set new high bars for Mg batteries in terms of energy, power, and cycle life

Dong et al., *Joule* 3, 782–793

March 20, 2019 © 2018 Elsevier Inc.

<https://doi.org/10.1016/j.joule.2018.11.022>



## Article

# Directing Mg-Storage Chemistry in Organic Polymers toward High-Energy Mg Batteries

Hui Dong,<sup>1</sup> Yanliang Liang,<sup>1,\*</sup> Oscar Tutasaus,<sup>2</sup> Rana Mohtadi,<sup>2</sup> Ye Zhang,<sup>1</sup> Fang Hao,<sup>1</sup> and Yan Yao<sup>1,3,\*</sup>

## SUMMARY

Magnesium batteries could offer high energy density and safety due to the non-dendritic Mg metal anode. However, Mg<sup>2+</sup> ingress into and diffusion within cathode materials are kinetically sluggish. It is therefore intriguing that recently organic cathodes were shown to deliver high energy and power even at room temperature. Herein we reveal that previous organic cathodes likely all operated on a MgCl-storage chemistry sustained by a large amount of electrolyte that significantly reduces cell energy. We then demonstrate Mg batteries featuring a Mg<sup>2+</sup>-storage chemistry using quinone polymer cathodes, chloride-free electrolytes, and a Mg metal anode. Under lean electrolyte conditions, the Mg<sup>2+</sup>-storing organic cathodes deliver the same energy while using ~10% of the amount of electrolyte needed for the MgCl-based counterparts. The observed specific energy (up to 243 Whr kg<sup>-1</sup>), power (up to 3.4 kW kg<sup>-1</sup>), and cycling stability (up to 87% at 2,500 cycles) of Mg-storage cells consolidate organic polymers as promising cathodes for high-energy Mg batteries.

## INTRODUCTION

Magnesium metal has the high capacity (2,205 mAh g<sup>-1</sup> and 3,833 mAh cm<sup>-3</sup>), low redox potential (-2.37 V versus normal hydrogen electrode), resource abundance, and non-dendritic deposition behavior to be qualified as an ideal anode for high-energy batteries.<sup>1</sup> A major challenge for realizing viable Mg batteries is the hunt for high-performance cathode materials that are chemically compatible with electrolytes in which highly reversible Mg deposition and stripping occur.<sup>2,3</sup> Magnesium ion has the radius of a Li ion but double the positive charge, and hence strong electrostatic interaction with anionic species in both electrolytes and cathode materials.<sup>4,5</sup> Both cleavage of Mg<sup>2+</sup> from solvated species such as Mg<sub>x</sub>Cl<sub>y</sub><sup>+</sup> before intercalation and solid-state Mg<sup>2+</sup> diffusion through negatively charged intercalation sites involve high energy barriers as a result.<sup>6-9</sup> The intercalation-type Mg-storage materials Chevrel phase Mo<sub>6</sub>S<sub>8</sub> and cubic Ti<sub>2</sub>S<sub>4</sub> deliver state-of-the-art specific energies of 140 and 212 Whr kg<sup>-1</sup> at elevated temperatures, respectively, but those values reduce to the less attractive 105 and 123 Whr kg<sup>-1</sup> at room temperature, respectively (Figure 1).<sup>10-12</sup> Other intercalation- and conversion-type compounds with high potential/specific capacity such as V<sub>2</sub>O<sub>5</sub><sup>13</sup> and sulfur<sup>14,15</sup> may become interesting candidates if compatibility with a Mg anode and a practical cell design become available.<sup>16</sup> Recently, multiple groups, including ours, have reported efficient Mg storage with organic electrode materials in both aqueous and non-aqueous electrolytes.<sup>17-22</sup> Some organic electrode materials, such as poly(1,4-anthraquinone) (P14AQ) and 2,5-dimethoxy-1,4-benzoquinone (DMBQ), deliver specific energies that match or exceed those by the best intercalation compounds even at room temperature in

## Context & Scale

Rechargeable Mg batteries are potentially safe and low-cost alternatives to lithium-ion batteries. One persistent challenge to the technology is the hunt for high-performance cathode materials. Even the most successful intercalation-type cathode materials deliver moderate energy and power only at elevated temperatures. Interestingly, several organic cathodes have been recently reported to show some of the highest energy and power, even at room temperature. In this work, we have scrutinized the charge storage mechanism of organic cathodes. We show that it is critical to rationally select the combination of electrolyte and organic cathode to direct the charge storage from a hybrid MgCl<sup>+</sup>-storage chemistry to genuine Mg<sup>2+</sup> storage, which is a prerequisite for a high-energy Mg battery. Two organic polymers are demonstrated to deliver some of the highest specific energy, power, and cycling stability for Mg batteries and are ready for integration into practically relevant cell design.



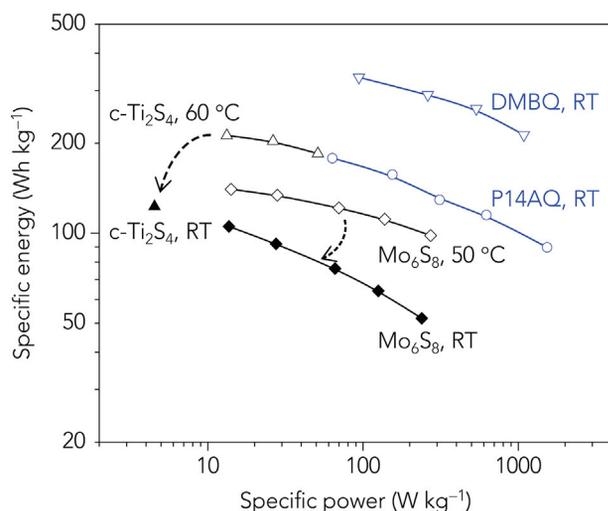


**Figure 1. Ragone Plot of Representative Mg Batteries**

Calculations are based on average discharge voltage and specific capacity considering only the weight of the cathode and anode active materials. For inorganic intercalation-type materials, values obtained at room temperature (RT) and elevated temperatures are both included as they usually vary considerably.<sup>11,12,17,19</sup> c-Ti<sub>2</sub>S<sub>4</sub>, cubic Ti<sub>2</sub>S<sub>4</sub>. The arrows indicate the performance degradation of a material when tested at a lower temperature.

similar Mg<sub>x</sub>Cl<sub>y</sub><sup>+</sup>-based electrolytes.<sup>17,19</sup> Such unique performance prompted us to scrutinize the Mg-storage chemistry and, more importantly, the practicality of organic carbonyl compounds as cathode materials for Mg batteries.

Herein we report the Mg-storage behavior of selected organic carbonyl compounds using a range of Mg metal-compatible electrolytes, based on which we propose a pathway toward high-energy organic Mg batteries. A vast library of organic carbonyl electrode materials is available thanks to active research on organic Li batteries,<sup>23–27</sup> among which three compounds are selected as model compounds: the small-molecule quinone DMBQ, which boasts high Li-storage specific capacity<sup>28</sup> and the highest specific energy for a Mg-storing organic cathode,<sup>17</sup> the polymeric quinone P14AQ, which shows relatively high specific energy and great cycling stability as both organic Li<sup>29</sup> and Mg<sup>19</sup> cathodes; and the conjugated redox polymer poly[[N,N'-bis(2-octyldodecyl)-1,4,5,8-naphthalenedicarboximide-2,6-diyl]-alt-5,5'-(2,2'-bithiophene)] (P(NDI2OD-T2)), which is a particularly fast and stable organic cathode for Li storage.<sup>30</sup> Quantitative elemental analysis reveals that, regardless of molecular structure or molecular weight, all three compounds predominantly store MgCl<sup>+</sup> instead of the previously assumed Mg<sup>2+</sup> when tested in Mg<sub>x</sub>Cl<sub>y</sub><sup>+</sup>-based electrolytes. Since the electrolyte is the sole supply of Cl, the MgCl-storage chemistry turns the electrolyte into an additional charge storage component alongside the cathode and anode. As such, this chemistry is not likely to allow for a lean-electrolyte cell design, which is crucial for a high-energy cell. However, we manage to enable a Mg-storage chemistry by electing chloride-free electrolytes with weakly coordinating bis(trifluoromethane)sulfonimide (TFSI)<sup>31</sup> and *closo*-carborane anions,<sup>32,33</sup> in which little or no anion co-storage with Mg<sup>2+</sup> is observed in our model polymers. The change from MgCl- to Mg-storage chemistry increases cell-level specific energy by multiple times, as explained theoretically by calculation and experimentally by cells using a limited amount of electrolyte (“lean electrolyte” conditions). Finally, through optimal combination of organic carbonyl polymer cathodes and Mg-storage-enabling electrolytes we

<sup>1</sup>Department of Electrical and Computer Engineering and Texas Center for Superconductivity, University of Houston, Houston, TX 77204, USA

<sup>2</sup>Materials Research Department, Toyota Research Institute of North America, Ann Arbor, MI 48105, USA

<sup>3</sup>Lead Contact

\*Correspondence: [yliang7@central.uh.edu](mailto:yliang7@central.uh.edu) (Y.L.), [yyao4@uh.edu](mailto:yyao4@uh.edu) (Y.Y.)

<https://doi.org/10.1016/j.joule.2018.11.022>

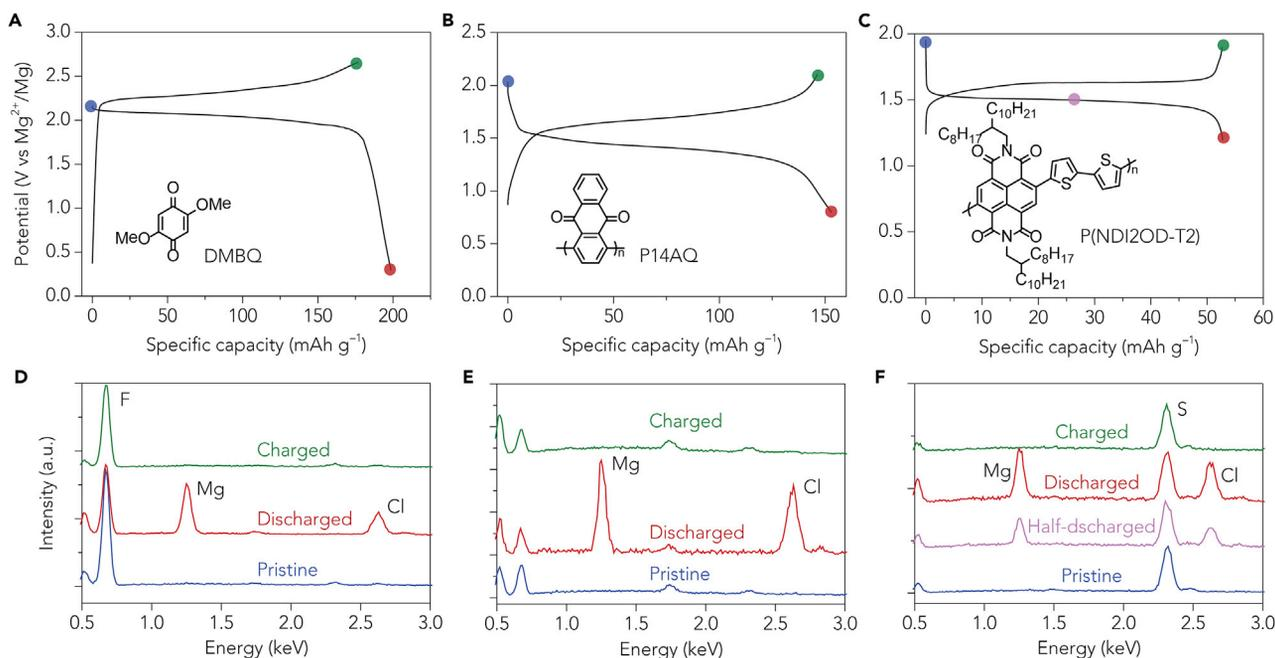


**Figure 2. Charge-Storage Mechanism of Organic Electrodes in Chloride-Containing Electrolytes**

(A–C) First-cycle galvanostatic discharge–charge voltage profiles of (A) DMBQ, (B) P14AQ, and (C) P(NDI2OD-T2). Current and electrolyte:  $150 \text{ mA g}^{-1}$ ,  $0.25 \text{ M Mg(TFSI)}_2$  and  $0.5 \text{ M MgCl}_2$  in DME for DMBQ;  $130 \text{ mA g}^{-1}$ ,  $0.3 \text{ M Mg(HMDS)}_2$  and  $1.2 \text{ M MgCl}_2$  in THF for P14AQ;  $11 \text{ mA g}^{-1}$ ,  $0.25 \text{ M Mg(TFSI)}_2$  and  $0.5 \text{ M MgCl}_2$  in DME for P(NDI2OD-T2).

(D–F) EDS spectra of (D) DMBQ, (E) P14AQ, and (F) P(NDI2OD-T2) electrodes at different states of charge corresponding to samples collected in (A)–(C).

are able to demonstrate high specific energy, power, and cycling stability that are rarely seen in Mg batteries.

## RESULTS AND DISCUSSION

Since a large variety of electrolytes are involved in this work, we performed cathode evaluation in three-electrode cells so that their voltage profiles were not obscured by any difference in the overpotential for Mg plating and stripping in different electrolytes. We first studied the charge-storage mechanism of the carbonyl compounds DMBQ, P14AQ, and P(NDI2OD-T2), the molecular structures of which are shown in Figure 2, in typical chloride-containing electrolytes.<sup>34,35</sup> DMBQ was originally reported in  $\text{Mg}(\text{ClO}_4)_2$ -butyrolactone and Mg-bis(trifluoromethanesulfonyl)amide-sulfone electrolytes, where DMBQ showed low potentials of  $\sim 1.1 \text{ V}$  versus  $\text{Mg}/\text{Mg}^{2+}$ .<sup>36,37</sup> The low potentials were interpreted as the result of the two chloride-free electrolytes being incompatible with Mg metal.<sup>17</sup> A recent reinvestigation of the molecule in  $\text{Mg}(\text{TFSI})_2$ - $2\text{MgCl}_2$  in dimethoxyethane (DME), an electrolyte capable of Mg metal plating and stripping,<sup>38</sup> revealed a clear discharge plateau at  $\sim 2 \text{ V}$  versus  $\text{Mg}/\text{Mg}^{2+}$  with specific capacity slightly above  $100 \text{ mAh g}^{-1}$  followed by a slope with another  $100 \text{ mAh g}^{-1}$ .<sup>17</sup> Here we investigated the material in the same electrolyte for a fair comparison but used the inert molybdenum (Mo) foil instead of stainless steel as the current collector for cleaner chemistry.<sup>39</sup> Figure 2A shows well-defined plateaus for both charge and discharge with specific capacity ( $200 \text{ mAh g}^{-1}$ ) similar to reported values. The DMBQ electrodes composed of DMBQ, conductive carbon, and polytetrafluoroethylene (PTFE) at pristine, discharged, and charged states were subjected to energy-dispersive X-ray spectroscopy (EDS) analysis. Strong Mg and Cl signals arose upon discharge, then both

vanished when charged (Figure 2D). The simultaneous appearance and disappearance of both signals indicate co-storage of the two elements. The presence or absence of TFSI<sup>-</sup> in the discharged sample cannot be confirmed due to the F signal arising from PTFE, but the possible TFSI<sup>-</sup> storage can be ruled out, as to be discussed later. The atomic ratio of Mg to Cl is 1:0.60 (with an error bar of  $\pm 4.1\%$ ), i.e., a split of ca. 2:3 between Mg<sup>2+</sup> and MgCl<sup>+</sup>. Therefore, the DMBQ | Mg(TFSI)<sub>2</sub>-2MgCl<sub>2</sub> | Mg battery is a hybrid-ion battery dominated by MgCl-ion storage rather than a Mg-ion battery.

Compared with molecular organic compounds, organic polymers are more popular cathode candidates due to their lower solubility in organic electrolytes. Therefore, we also studied P14AQ as a representative polymer cathode. Another Mg metal-compatible electrolyte, Mg(HMDS)<sub>2</sub>-4MgCl<sub>2</sub> (HMDS = hexamethyldisilazide) in tetrahydrofuran (THF), was used following a previous report.<sup>40</sup> The polymer showed a sloping plateau during both charge and discharge with a specific capacity of 155 mAh g<sup>-1</sup> at an average of  $\sim 1.36$  V versus Mg/Mg<sup>2+</sup> (Figure 2B), agreeing well with the previous report.<sup>19</sup> Both Mg and Cl signals were again observed in the discharged electrode, with the atomic ratio of Mg:Cl being 1:0.97 (with an error bar of  $\pm 4.3\%$ ), indicating almost exclusive MgCl<sup>+</sup> storage.

The S-containing carbonyl polymer P(NDI2OD-T2) provides more insight into the electrode reaction. According to previous studies of the polymer for Li batteries, each repeating NDI2OD-T2 unit reversibly stores two electrons, corresponding to a theoretical capacity of 54.2 mAh g<sup>-1</sup>.<sup>30</sup> The polymer showed flat plateaus for both charge and discharge with a small overpotential of 133 mV. The observed specific capacity of 52.8 mAh g<sup>-1</sup> corresponds to 97% of its theoretical capacity. Such high level of material utilization is a major improvement from the previous reports (<70%)<sup>18</sup> and implies that there is no fundamental limitation for an organic electrode material to achieve designed capacity. Binder-free electrodes composed of P(NDI2OD-T2) and conductive carbon were tested in a Mg(TFSI)<sub>2</sub>-2MgCl<sub>2</sub> electrolyte (same as that for DMBQ) and analyzed with EDS. When half-discharged, the atomic ratio of Mg:Cl:S was 1:0.96:1.97 (with an error bar of  $\pm 4.3\%$ ), i.e., each electron injected into the polymer is balanced by a MgCl<sup>+</sup> ion. As discharge completed, both Mg and Cl amounts doubled, and the ratio became 1:0.96:0.99 (with an error bar of  $\pm 3.2\%$ ). Upon charge, both Mg and Cl signals disappeared, leaving only S of the bithiophene moiety. No F signal was detected throughout the cycle even though there are TFSI<sup>-</sup> ions in the electrolyte. We conclude that both polymers underwent MgCl<sup>+</sup> storage regardless of the redox-active core (quinone versus imide), solvent (THF versus DME), and anion species (HMDS<sup>-</sup> versus TFSI<sup>-</sup>). On the basis of the fact that all previously reported organic Mg batteries use quinone and imide molecule/polymer cathodes and chloride-containing ethereal electrolytes, we believe what were assumed to be organic "Mg-ion" cathodes and batteries all involve MgCl-storage chemistry.

A hybrid-ion cell design where the cathode and anode store different ions (MgCl<sup>+</sup> and Mg<sup>2+</sup> in this case) offers plenty of flexibility in choice of electrode chemistry and has enabled many interesting types of batteries.<sup>41-44</sup> However, the reliance on extra electrolytes dedicated to ion storage, as will be demonstrated later, makes such design unlikely to compete as a high-energy battery. We have therefore explored the plausibility of true organic Mg-ion batteries by using chloride-free Mg metal-compatible electrolytes. Figure 3A shows such an example using a P(NDI2OD-T2) cathode and a Mg(TFSI)<sub>2</sub>/diglyme electrolyte. This very simple electrolyte, when dried thoroughly, allows reversible Mg plating and stripping with a

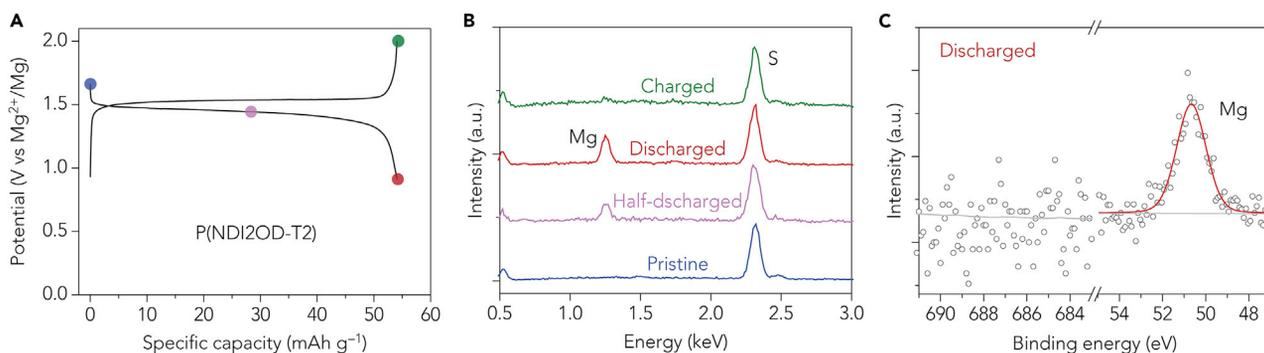


**Figure 3. Charge Storage Mechanism of P(NDI2OD-T2) in Chloride-Free Electrolytes**

(A) First-cycle galvanostatic discharge–charge voltage profile of P(NDI2OD-T2). Current and electrolyte: 11 mA g<sup>-1</sup>, 0.2 M Mg(TFSI)<sub>2</sub> in diglyme. (B) EDS spectra of P(NDI2OD-T2) electrodes at different states of charge corresponding to samples collected in (A). (C) X-ray photoelectron spectroscopy spectrum of F 1s and Mg 2p for discharged P(NDI2OD-T2) electrode. The discharged sample is confirmed absence of F (689 eV).

surprisingly decent coulombic efficiency of 98.8% albeit a large overpotential for stripping (Figure S1). It makes for an economic model electrolyte for our three-electrode cells where a large amount of electrolyte is required and the anode overpotential does not obscure the cathode profile. P(NDI2OD-T2) again showed flat plateaus with small polarization (91 mV) and 99.8% material utilization (54.1 mAh g<sup>-1</sup>). EDS analysis showed Mg:S ratios of 1:3.81 (with an error bar of ±4.4%) and 1:2.01 (with an error bar of ±3.1%) for the half-discharged and fully discharged states, respectively, and no F signal throughout the cycle (Figure 3B). The results indicate no anion co-storage, and each Mg<sup>2+</sup> balances two negative charges. X-ray photoelectron spectroscopy analysis of the discharged sample also confirmed the absence of F (689 eV) in Figure 3C. Another example involved a P(NDI2OD-T2) cathode and a Mg(CB<sub>11</sub>H<sub>12</sub>)<sub>2</sub>/tetraglyme electrolyte, which showed efficient Mg plating and stripping.<sup>32</sup> The monocarborane anion CB<sub>11</sub>H<sub>12</sub><sup>-</sup> is non-corrosive, chemically inert, and, most importantly, weakly coordinating. P(NDI2OD-T2) shows slightly larger polarization (151 mV) and lower specific capacity (50.5 mAh g<sup>-1</sup>) in this electrolyte, most likely due to the high viscosity of tetraglyme (Figure S2). The discharged electrode had a Mg:B:S ratio of 1:2.21:1.93 according to inductively coupled plasma spectroscopy. The atomic ratio does not allow us to mathematically determine whether the B existed as the hybrid ion Mg(CB<sub>11</sub>H<sub>12</sub>)<sup>+</sup> or residual solute Mg(CB<sub>11</sub>H<sub>12</sub>)<sub>2</sub>. If all B entered the polymer as Mg(CB<sub>11</sub>H<sub>12</sub>)<sup>+</sup>, the ratio of Mg<sup>2+</sup> and Mg(CB<sub>11</sub>H<sub>12</sub>)<sup>+</sup> would be ca. 4:1, i.e., Mg<sup>2+</sup> being the dominant storage species. However, considering the fact that the more strongly coordinating TFSI<sup>-</sup> anions did not enter the polymer as Mg(TFSI)<sup>+</sup>, the possibility of Mg(CB<sub>11</sub>H<sub>12</sub>)<sup>+</sup> is less likely.<sup>31,45</sup> Instead, residual Mg(CB<sub>11</sub>H<sub>12</sub>)<sub>2</sub> is the more likely source of B due to the difficulty in thoroughly washing the very viscous electrolyte from the polymer electrode. The above two examples indicate the plausibility of having a Mg<sup>2+</sup>-storing organic cathode in a Mg metal-compatible electrolyte.

The ion storage chemistry has an immense impact on the specific energy of a battery. Figures 4A and 4B compare the reaction and mass flux in Mg batteries based on MgCl- and Mg-storage chemistries, respectively. During the discharge of a MgCl-storage cell, a Mg atom in the Mg metal anode loses two electrons and enters the electrolyte as Mg<sup>2+</sup>. Mg<sup>2+</sup> then accepts a Cl<sup>-</sup> from the MgCl<sub>2</sub> in the electrolyte and forms MgCl<sup>+</sup>, which enters the cathode as monovalent cations. Since the cathode stores both Mg<sup>2+</sup> and Cl<sup>-</sup> but the anode stores only Mg, the electrolyte has to double as a Cl<sup>-</sup> reservoir (in addition to ion conduction), and the amount of Cl<sup>-</sup> in the

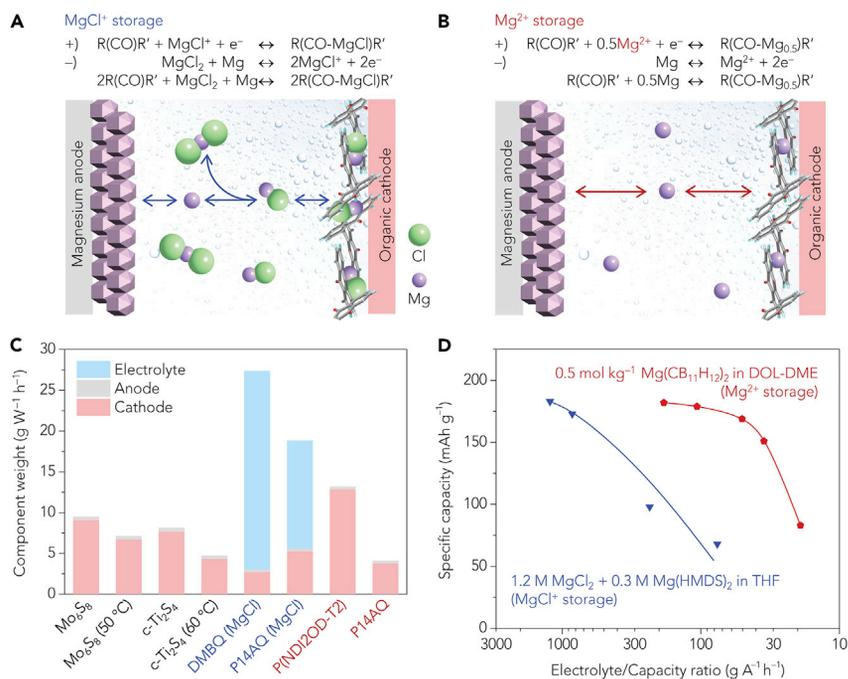


**Figure 4. Impact of MgCl<sup>-</sup> and Mg-Storage Chemistries on Cell Specific Energy**

(A and B) Reaction equations and schematic illustrations of the working mechanism of organic cathodes in (A) chloride-containing and (B) chloride-free electrolytes. (C) Breakdown of the weights of cathode material, anode material, and electrolyte (both solute and solvent) per watt hour for representative Mg battery chemistries (stoichiometric amount of each component was considered).<sup>11,12,17,19</sup> (D) Comparison of P14AQ-Mg cells in electrolytes containing MgCl<sup>+</sup> and Mg<sup>2+</sup> under lean electrolyte conditions as a function of the electrolyte:capacity (E:C) ratio. “E” represents the mass of electrolyte used in a cell, and “C” is the designed capacity based on a specific capacity of 193 mAh g<sup>-1</sup> for P14AQ. Refer to Figure S4 for voltage profiles.

electrolyte must at least match the capacity of the cathode. The Mg-storage scenario is a much simpler rocking chair mechanism where a flux of Mg<sup>2+</sup> goes from the anode to the cathode during discharge and vice versa. Minimal electrolyte is needed to provide ionic conduction between the two electrodes.

One way to visualize the impact of the storage chemistry on cell energy is to look at the weight of materials needed to achieve a given energy. Figure 4C breaks down the weights of cathode material, anode material, and electrolyte (both solute and solvent) per watt hour for some representative Mg-battery chemistries. The weight of anode material, i.e., Mg metal, is marginal in all cases due to its high specific capacity. The thio spinel Ti<sub>2</sub>S<sub>4</sub> operated at 60 °C takes less than 5 g of electrode materials to achieve 1 Whr. The previously reported organic cathodes P14AQ and DMBQ, when considering a solely MgCl-storage mechanism, suffer significantly from the massive weight of electrolyte. The situation is worse for DMBQ than for P14AQ due to a less concentrated MgCl<sub>2</sub> being used for the former (0.5 versus 1.2 M). While it is possible to reduce the electrolyte amount by increasing the MgCl<sub>2</sub> concentration, the limited solubility of MgCl<sub>2</sub> would eventually become the limiting factor. Similar discussions on the energy limitation by electrolyte had been made for hybrid-ion battery chemistries such as Mg<sup>2+</sup>-Li<sup>+</sup>/Na<sup>+</sup> hybrid batteries<sup>46,47</sup> and AlCl<sub>4</sub><sup>-</sup>-based Al batteries.<sup>48</sup> These batteries could theoretically use much more concentrated electrolytes, but the weight of electrolyte was still found to be the

main limit on practical cell energy. Moving from MgCl<sup>-</sup> to Mg-storage chemistry trims the electrolyte from energy storage components, enabling P14AQ–Mg to be one of the highest-energy Mg batteries.

The above analysis assumes the cell operation is sustained as long as the MgCl-storage chemistry is stoichiometrically satisfied. In practice, all Cl<sup>-</sup> stored in the electrolyte cannot be consumed before the cell fails, because an appropriate concentration of Cl<sup>-</sup> is necessary to keep up the reversibility of Mg plating and stripping.<sup>49</sup> To develop a more realistic understanding of the impact of the hybrid-ion chemistry on cell energy, we have compared P14AQ–Mg cells in electrolytes containing MgCl<sup>+</sup> and Mg<sup>2+</sup> under lean electrolyte conditions (Figure 4D). Electrodes with high areal loading (5 mg cm<sup>-2</sup>) were used to better reflect a real-world application scenario. Mg(HMDS)<sub>2</sub>–4MgCl<sub>2</sub> with a relatively high MgCl<sub>2</sub> concentration was used for the MgCl<sup>+</sup> cell. The Mg<sup>2+</sup> cell employed a low-viscosity monocarborane electrolyte by replacing tetraglyme with a mixture of 1,3-dioxolane and DME (Figure S3). The polymer delivered the same maximum capacity of ~180 mAh g<sub>P14AQ</sub><sup>-1</sup> in both electrolytes when the electrolyte is abundant. As we reduced the electrolyte:capacity ratio (E:C ratio, in g A<sup>-1</sup> hr<sup>-1</sup>) by decreasing the amount of electrolyte, the capacities of both cells dropped. To deliver 90% and 50% of the maximum capacity, the MgCl<sup>+</sup> cell required 620 and 142 g A<sup>-1</sup> hr<sup>-1</sup> of electrolyte, respectively, while the Mg<sup>2+</sup> cell required 41 and 20 g A<sup>-1</sup> hr<sup>-1</sup>, respectively. That is, the Mg<sup>2+</sup> cell needs about 1 order of magnitude less electrolyte to deliver the same capacity. To put it into context, a Li–S cell with an electrolyte:sulfur ratio (in g g<sup>-1</sup>) of 12, a common lean electrolyte condition, has an E:C ratio of 15 g A<sup>-1</sup> hr<sup>-1</sup> considering a specific capacity of 800 mAh g<sup>-1</sup>.<sup>50</sup> To the best of our knowledge, this is the first report on a Mg battery operated with a limited amount of electrolyte. We expect higher capacity at lower E:C ratio when dedicated efforts are made to optimize electrode and cell fabrication.

We have studied the rate capability and cycling performance of P(NDI2OD-T2) and P14AQ in greater detail. P(NDI2OD-T2) showed excellent fast charge–discharge performance with well-defined plateaus and 70% of theoretical specific capacity maintained at 50 C (1 C = 54 mA g<sup>-1</sup>) (Figure 5A). P14AQ showed two plateaus as opposed to one as observed in chloride-containing electrolytes; the polymer also showed one plateau for Li<sup>+</sup> storage;<sup>29</sup> therefore, the difference in plateau number may be intrinsic to the valence of ions stored. The performance of P14AQ is more sensitive to current density, but the maximum specific power of 553 W kg<sup>-1</sup> is still appreciable especially considering this result is obtained at room temperature (Figure 5B). Figure 5C compares the energy and power of cells operated on the two storage chemistries. When the specific capacities of cells obtained from electrolytes containing MgCl<sup>+</sup> are calculated based on the weight of the electrode materials, the specific energies of the DMBQ–Mg<sup>2+</sup> and P14AQ–Mg<sup>2+</sup> cells both appear pretty high (light blue in Figure 5C). Once the MgCl-storage mechanism and the weight of the theoretically required amount of electrolyte are considered, the specific energies of DMBQ–MgCl and P14AQ–MgCl (deep blue) drop well below those achieved by inorganic intercalation compounds. The specific energies of the Mg-storage P(NDI2OD-T2)–Mg<sup>2+</sup> and P14AQ–Mg<sup>2+</sup> cells are not discounted by electrolytes (red). The P14AQ–Mg<sup>2+</sup> cells show specific energies of up to 243 Whr kg<sup>-1</sup>, while the P(NDI2OD-T2)–Mg<sup>2+</sup> cells show specific powers of up to 3.4 kW kg<sup>-1</sup>. Both P(NDI2OD-T2) and P14AQ showed stable cycling performance. P(NDI2OD-T2) maintained 87% of its initial capacity after 2500 deep cycles (>700 hr), representing one of the most stable cycling performances for a non-aqueous Mg battery. P14AQ stabilized at ~130 mAh g<sup>-1</sup> after decay in the initial ~10 cycles. After

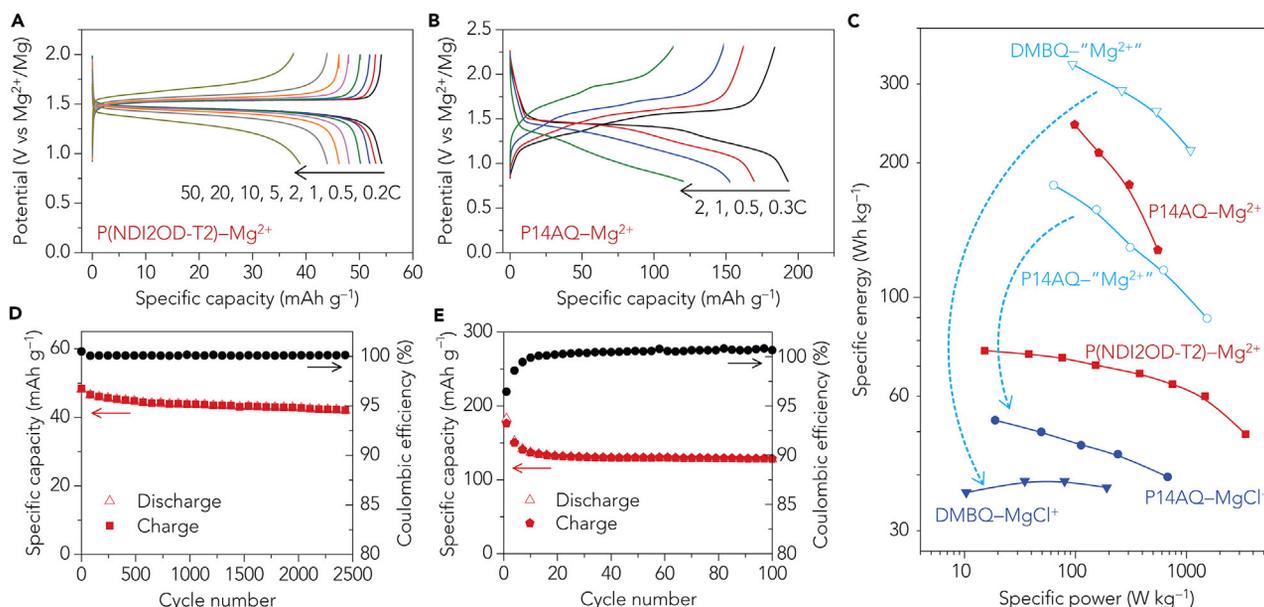


**Figure 5. Electrochemical Performance of Organic Mg-Ion Batteries**

(A and B) Voltage profiles of (A) P(NDI2OD-T2) and (B) P14AQ at different current densities. Electrolyte: 0.2 M Mg(TFSI)<sub>2</sub> in diglyme. The arrows indicate the change of profiles with increasing current density.

(C) Ragone plot of organic Mg batteries with different ion-storage mechanisms. Refer to [Experimental Procedures](#) for calculation details. The specific energies of the DMBQ-“Mg<sup>2+</sup>” and P14AQ-“Mg<sup>2+</sup>” cells seem very high (light blue).<sup>17,19</sup> When the MgCl-storage mechanism and the weight of the theoretically required amount of electrolyte are considered, the specific energies of DMBQ-MgCl and P14AQ-MgCl are discounted by multiple times (deep blue). The specific energies of the Mg-storage P(NDI2OD-T2)-Mg<sup>2+</sup> and P14AQ-Mg<sup>2+</sup> cells are not discounted by electrolytes (red).

(D and E) Cycling stability and coulombic efficiency of (D) P(NDI2OD-T2) and (E) P14AQ cycled at the current density of 300 and 130 mA g<sup>-1</sup>, respectively. Red symbols indicate specific capacity; black symbols indicate coulombic efficiency.

10 cycles, the average coulombic efficiency is slightly beyond unity at 100.5%, which we ascribe to a shuttle effect due to the slight dissolution of P14AQ.

In summary, we have evaluated the suitability of organic compounds as cathode materials for high-energy Mg batteries. We have identified that in typical chloride-containing electrolytes, storage of MgCl<sup>+</sup> is dominant in probably all organic electrode materials, hence previously assumed organic “Mg-ion” electrodes and batteries are indeed hybrid-ion ones. The negative impact of the hybrid-ion-storage chemistry on the cell specific energy was elucidated through theoretical analysis and cell tests with controlled amount of electrolyte. We further showed that with the right combination of organic cathodes and chloride-free electrolytes, storage of Mg<sup>2+</sup> in organic electrodes is possible without compromising the reversibility of Mg metal plating and stripping and the energy and power of the cell. Preliminary results from lean electrolyte cells indicate the plausibility of organic Mg batteries being designed as practical high-energy storage devices. With the help of the Mg-storage chemistry, organic polymers have delivered some of the highest specific energy, power, and cycling stability for Mg batteries. Going forward, designing electrodes with higher mass loading, higher active material ratio, and lower electrolyte demand would be just as important as developing better cathode materials for achieving truly high practical cell specific energy.

## EXPERIMENTAL PROCEDURES

### Fabrication of Organic Electrodes

Electrode compositions and preparation methods followed previous reports for DMBQ,<sup>17</sup> P14AQ,<sup>19</sup> and P(NDI2OD-T2) for fair comparison.<sup>30</sup> For lean electrolyte tests, we increased the ratio of the active material to avoid unnecessary electrolyte

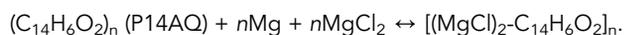
take-up by inactive components. The preparation of P(NDI2OD-T2) electrodes followed previous binder-free procedures for the same polymer.<sup>30</sup> P(NDI2OD-T2) and Super-P carbon were hand ground with a pestle and mortar at a mass ratio of 6:4 with the aid of 1,2-dichlorobenzene without the use of binder. The resulting slurry was spread onto stainless steel foil current collectors. The preparation of P14AQ and DMBQ electrodes followed a binder-assisted procedure for quinone electrodes.<sup>20</sup> P14AQ, Super-P carbon, and PTFE binder were mixed in a 4:5:1 ratio with the aid of ethanol and pressed into stainless steel mesh. DMBQ, Super-P carbon, and PTFE binder were mixed in a 5:4:1 ratio with the aid of ethanol and pressed on a Mo foil. Mo foils were used due to its anti-corrosion property at high charging potentials. The areal mass loading of active materials is  $1 \text{ mg cm}^{-2}$  in this work unless otherwise indicated. For the experiment on the effect of the electrolyte amount on the capacity, P14AQ, Super-P carbon, and PTFE binder were mixed in a 6:3:1 ratio and the areal mass loading of P14AQ in the electrode was  $5 \text{ mg cm}^{-2}$ . All electrodes were dried at  $100^\circ\text{C}$  under vacuum for 6 hr and used without being calendared.

### Electrochemical Measurements

Tubular hermetically sealed three-electrode cells<sup>46</sup> were used for all electrochemical characterizations except for lean electrolyte tests, for which two-electrode coin cells were used. The three-electrode cells require such a large amount of electrolyte (testing setup shown in Yoo et al.<sup>46</sup>) that we decided to use the affordable  $\text{Mg}(\text{TFSI})_2/\text{diglyme}$  as a model electrolyte for the chloride-free scenario. Practical batteries are expected to be, instead, fabricated using two-electrode cells, in which a small amount of electrolyte is needed and the use of the optimal  $\text{Mg}(\text{CB}_{11}\text{H}_{12})_2/\text{tetraglyme}$  electrolyte, in which the overpotential for Mg plating and stripping is small,<sup>32</sup> becomes economically viable. The two electrolytes share high-efficiency Mg plating and stripping and chloride-free electrolyte, with the only difference being the anode overpotential. All cells were assembled in an Ar-filled glove box (MBRAUN, Garching, Germany), and electrochemical characterizations were conducted using a potentiostat (VMP-3, Bio-Logic, Claix, France). For the three-electrode setup, the electrodes of interest were used as working electrodes. Freshly polished magnesium foils ( $50 \mu\text{m}$  thick, 99.95%, GalliumSource, Scotts Valley, CA) were used as both counter and reference electrodes. The capacity of the Mg anode is greater than that of the cathode. A trilayer polypropylene/polyethylene/polypropylene separator ( $25 \mu\text{m}$  thick, Celgard 2325, Celgard) was used in coin cells.

### Specific Energy Calculations

For cells using chloride-containing electrolytes, the calculation is based on the following reaction equations:



The cell specific energy ( $E_s$ ) is calculated as

$$E_s = E \times (C_c^{-1} + C_a^{-1} + C_e^{-1})^{-1},$$

where  $E$  is the average discharge voltage,  $C_c$  is cathode specific capacity,  $C_a$  is anode specific capacity, and  $C_e$  is the apparent specific capacity of the electrolyte defined as

$$C_e = z \times F \times (M_w \times c^{-1})^{-1},$$

where  $M_w$  is the molecular weight of the solute that participates in the reaction ( $\text{MgCl}_2$  here),  $z$  is the mole number of electrons transferred with the consumption of 1 mol of electrolyte solute molecule ( $z = 2$  for both reactions),  $F$  is the Faraday constant, and  $c$  is the weight percentage of the solute ( $\text{MgCl}_2$ ) in the electrolyte. For cells using chloride-free electrolytes,  $C_e$  is taken out of the equation

$$E_s = E \times (C_c^{-1} + C_a^{-1})^{-1}.$$

The values of  $E$  were taken from the corresponding reports, which were typically obtained in two-electrode cells. For polymer cells based on Mg-storage chemistry, the  $E$  values were taken from three-electrode cells shown in Figure 5. The use of cathode discharge potential obtained from three-electrode cells as discharge voltage omits the stripping overpotential of Mg metal; this is sufficiently small (e.g., 49 mV at  $0.1 \text{ mA cm}^{-2}$ , see Figure S2) compared with the polymer cathode potential. The performance parameters of cells based on MgCl- and Mg-storage chemistries are summarized in Tables S1 and S2, respectively.

## SUPPLEMENTAL INFORMATION

Supplemental Information includes Supplemental Experimental Procedures, four figures, and two tables and can be found with this article online at <https://doi.org/10.1016/j.joule.2018.11.022>.

## ACKNOWLEDGMENTS

Y.Y. acknowledges funding support from the US Department of Energy's Office of Energy Efficiency and Renewable Energy (EERE), as part of the Battery 500 Consortium (Award No. DE-EE0008234). We appreciate Professor Antonio Facchetti from Northwestern University for providing the P(NDI2OD-T2) polymer used in this study.

## AUTHOR CONTRIBUTIONS

Y.Y. conceived the study and supervised the project. Y.L. and H.D. designed the experiments. H.D. performed electrochemical and material characterizations. O.T., R.M., and H.D. synthesized the electrolytes. Y.Z. and F.H. assisted in cell fabrication. Y.L., H.D., and Y.Y. wrote the manuscript. All authors commented on the results and the manuscript.

## DECLARATION OF INTERESTS

Yan Yao is a founder of Polymax Energy, Inc.

Received: September 21, 2018

Revised: October 26, 2018

Accepted: November 27, 2018

Published: December 21, 2018

## REFERENCES

1. Yoo, H.D., Shterenberg, I., Gofer, Y., Gershinsky, G., Pour, N., and Aurbach, D. (2013). Mg rechargeable batteries: an on-going challenge. *Energy Environ. Sci.* *6*, 2265–2279.
2. Canepa, P., Sai Gautam, G., Hannah, D.C., Malik, R., Liu, M., Gallagher, K.G., Persson, K.A., and Ceder, G. (2017). Odyssey of multivalent cathode materials: open questions and future challenges. *Chem. Rev.* *117*, 4287–4341.
3. Muldoon, J., Bucur, C.B., and Gregory, T. (2017). Fervent hype behind magnesium batteries: an open call to synthetic chemists—electrolytes and cathodes needed. *Angew. Chem. Int. Ed.* *56*, 12064–12084.
4. Canepa, P., Jayaraman, S., Cheng, L., Rajput, N.N., Richards, W.D., Gautam, G.S., Curtiss, L.A., Persson, K.A., and Ceder, G. (2015).

- Elucidating the structure of the magnesium aluminum chloride complex electrolyte for magnesium-ion batteries. *Energy Environ. Sci.* **8**, 3718–3730.
- Liang, Y.L., Yoo, H.D., Li, Y.F., Shuai, J., Calderon, H.A., Hernandez, F.C.R., Grabow, L.C., and Yao, Y. (2015). Interlayer-expanded molybdenum disulfide nanocomposites for electrochemical magnesium storage. *Nano Lett.* **15**, 2194–2202.
  - Wan, L.W.F., Perdue, B.R., Apblett, C.A., and Prendergast, D. (2015). Mg desolvation and intercalation mechanism at the  $\text{Mo}_6\text{S}_8$  Chevrel phase surface. *Chem. Mater.* **27**, 5932–5940.
  - Yoo, H.D., Liang, Y.L., Dong, H., Lin, J.H., Wang, H., Liu, Y.S., Ma, L., Wu, T.P., Li, Y.F., Ru, Q., et al. (2017). Fast kinetics of magnesium monochloride cations in interlayer-expanded titanium disulfide for magnesium rechargeable batteries. *Nat. Commun.* **8**, 339.
  - Sun, X., Duffort, V., Mehdi, B.L., Browning, N.D., and Nazar, L.F. (2016). Investigation of the mechanism of Mg insertion in birnessite in nonaqueous and aqueous rechargeable Mg-ion batteries. *Chem. Mater.* **28**, 534–542.
  - Zhou, L., Liu, Q., Zhang, Z., Zhang, K., Xiong, F., Tan, S., An, Q., Kang, Y.M., Zhou, Z., and Mai, L. (2018). Interlayer-spacing-regulated  $\text{VOPO}_4$  nanosheets with fast kinetics for high-capacity and durable rechargeable magnesium batteries. *Adv. Mater.* **30**, 1801984.
  - Aurbach, D., Lu, Z., Schechter, A., Gofer, Y., Gizbar, H., Turgeman, R., Cohen, Y., Moshkovich, M., and Levi, E. (2000). Prototype systems for rechargeable magnesium batteries. *Nature* **407**, 724–727.
  - Sun, X.Q., Bonnick, P., Duffort, V., Liu, M., Rong, Z.Q., Persson, K.A., Ceder, G., and Nazar, L.F. (2016). A high capacity thiospinel cathode for Mg batteries. *Energy Environ. Sci.* **9**, 2273–2277.
  - Liao, C., Guo, B., Jiang, D.-E., Custelcean, R., Mahurin, S.M., Sun, X.-G., and Dai, S. (2014). Highly soluble alkoxide magnesium salts for rechargeable magnesium batteries. *J. Mater. Chem. A* **2**, 581–584.
  - Andrews, J.L., Mukherjee, A., Yoo, H.D., Parija, A., Marley, P.M., Fakra, S., Prendergast, D., Cabana, J., Klie, R.F., and Banerjee, S. (2018). Reversible Mg-ion insertion in a metastable one-dimensional polymorph of  $\text{V}_2\text{O}_5$ . *Chem* **4**, 564–585.
  - Zhang, Z., Cui, Z., Qiao, L., Guan, J., Xu, H., Wang, X., Hu, P., Du, H., Li, S., Zhou, X., et al. (2017). Novel design concepts of efficient Mg-ion electrolytes toward high-performance magnesium-selenium and magnesium-sulfur batteries. *Adv. Energy Mater.* **7**, 1602055.
  - Zhao-Karger, Z., Zhao, X., Wang, D., Diemant, T., Behm, R.J., and Fichtner, M. (2015). Performance improvement of magnesium sulfur batteries with modified non-nucleophilic electrolytes. *Adv. Energy Mater.* **5**, 1401155.
  - Salama, M., Attias, R., Hirsch, B., Yemini, R., Gofer, Y., Noked, M., and Aurbach, D. (2018). On the feasibility of practical Mg-S batteries: practical limitations associated with metallic magnesium anodes. *ACS Appl. Mater. Interfaces* **10**, 36910–36917.
  - Pan, B.F., Zhou, D.H., Huang, J.H., Zhang, L., Burrell, A.K., Vaughey, J.T., Zhang, Z.C., and Liao, C. (2016). 2,5-Dimethoxy-1,4-benzoquinone (DMBQ) as organic cathode for rechargeable magnesium-ion batteries. *J. Electrochem. Soc.* **163**, A580–A583.
  - Bitenc, J., Pirnat, K., Bancic, T., Gaberscek, M., Genorio, B., Randon-Vitanova, A., and Dominko, R. (2015). Anthraquinone-based polymer as cathode in rechargeable magnesium batteries. *ChemSusChem* **8**, 4128–4132.
  - Pan, B.F., Huang, J.H., Feng, Z.X., Zeng, L., He, M.N., Zhang, L., Vaughey, J.T., Bedzyk, M.J., Fenter, P., Zhang, Z.C., et al. (2016). Polyanthraquinone-based organic cathode for high-performance rechargeable magnesium-ion batteries. *Adv. Energy Mater.* **6**, 1600140.
  - Liang, Y.L., Jing, Y., Gheyfani, S., Lee, K.Y., Liu, P., Facchetti, A., and Yao, Y. (2017). Universal quinone electrodes for long cycle life aqueous rechargeable batteries. *Nat. Mater.* **16**, 841–848.
  - Fan, X., Wang, F., Ji, X., Wang, R., Gao, T., Hou, S., Chen, J., Deng, T., Li, X., Chen, L., et al. (2018). A universal organic cathode for ultrafast lithium and multivalent metal batteries. *Angew. Chem. Int. Ed.* **57**, 7146–7150.
  - Chen, L., Bao, J.L., Dong, X., Truhlar, D.G., Wang, Y., Wang, C., and Xia, Y. (2017). Aqueous Mg-ion battery based on polyimide anode and Prussian blue cathode. *ACS Energy Lett.* **2**, 1115–1121.
  - Liang, Y.L., Tao, Z.L., and Chen, J. (2012). Organic electrode materials for rechargeable lithium batteries. *Adv. Energy Mater.* **2**, 742–769.
  - Poizot, P., and Dolhem, F. (2011). Clean energy new deal for a sustainable world: from non- $\text{CO}_2$  generating energy sources to greener electrochemical storage devices. *Energy Environ. Sci.* **4**, 2003–2019.
  - Song, Z., and Zhou, H. (2013). Towards sustainable and versatile energy storage devices: an overview of organic electrode materials. *Energy Environ. Sci.* **6**, 2280–2301.
  - Zhao, Q., Zhu, Z., and Chen, J. (2017). Molecular engineering with organic carbonyl electrode materials for advanced stationary and redox flow rechargeable batteries. *Adv. Mater.* **29**, 1607007.
  - Liang, Y., and Yao, Y. (2018). Positioning organic electrode materials in the battery landscape. *Joule* **2**, 1690–1706.
  - Yao, M., Senoh, H., Yamazaki, S.-I., Siroma, Z., Sakai, T., and Yasuda, K. (2010). High-capacity organic positive-electrode material based on a benzoquinone derivative for use in rechargeable lithium batteries. *J. Power Sources* **195**, 8336–8340.
  - Song, Z., Qian, Y., Gordin, M.L., Tang, D., Xu, T., Otani, M., Zhan, H., Zhou, H., and Wang, D. (2015). Polyanthraquinone as a reliable organic electrode for stable and fast lithium storage. *Angew. Chem. Int. Ed.* **54**, 13947–13951.
  - Liang, Y.L., Chen, Z.H., Jing, Y., Rong, Y.G., Facchetti, A., and Yao, Y. (2015). Heavily n-dopable  $\pi$ -conjugated redox polymers with ultrafast energy storage capability. *J. Am. Chem. Soc.* **137**, 4956–4959.
  - Sa, N., Rajput, N.N., Wang, H., Key, B., Ferrandon, M., Srinivasan, V., Persson, K.A., Burrell, A.K., and Vaughey, J.T. (2016). Concentration dependent electrochemical properties and structural analysis of a simple magnesium electrolyte: magnesium bis(trifluoromethane sulfonyl)imide in diglyme. *RSC Adv.* **6**, 113663–113670.
  - Tutusaus, O., Mohtadi, R., Arthur, T.S., Mizuno, F., Nelson, E.G., and Sevryugina, Y.V. (2015). An efficient halogen-free electrolyte for use in rechargeable magnesium batteries. *Angew. Chem. Int. Ed.* **54**, 7900–7904.
  - Hahn, N.T., Seguin, T.J., Lau, K.C., Liao, C., Ingram, B.J., Persson, K.A., and Zavadil, K.R. (2018). Enhanced stability of the carba-dodecaborate anion for high-voltage battery electrolytes through rational design. *J. Am. Chem. Soc.* **140**, 11076–11084.
  - He, S.J., Nielson, K.V., Luo, J., and Liu, T.L. (2017). Recent advances on  $\text{MgCl}_2$  based electrolytes for rechargeable Mg batteries. *Energy Storage Mater.* **8**, 184–188.
  - Barile, C.J., Barile, E.C., Zavadil, K.R., Nuzzo, R.G., and Gewirth, A.A. (2014). Electrolytic conditioning of a magnesium aluminum chloride complex for reversible magnesium deposition. *J. Phys. Chem. C* **118**, 27623–27630.
  - Sano, H., Senoh, H., Yao, M., Sakaebe, H., and Kiyobayashi, T. (2012).  $\text{Mg}^{2+}$  storage in organic positive-electrode active material based on 2,5-dimethoxy-1,4-benzoquinone. *Chem. Lett.* **41**, 1594–1596.
  - Senoh, H., Sakaebe, H., Sano, H., Yao, M., Kuratani, K., Takeichi, N., and Kiyobayashi, T. (2014). Sulfone-based electrolyte solutions for rechargeable magnesium batteries using 2,5-dimethoxy-1,4-benzoquinone positive electrode. *J. Electrochem. Soc.* **161**, A1315–A1320.
  - Shterenberg, I., Salama, M., Yoo, H.D., Gofer, Y., Park, J.B., Sun, Y.K., and Aurbach, D. (2015). Evaluation of  $(\text{CF}_3\text{SO}_2)_2\text{N}^-$  (TFSI) based electrolyte solutions for Mg batteries. *J. Electrochem. Soc.* **162**, A7118–A7128.
  - Cheng, Y.W., Liu, T.B., Shao, Y.Y., Engelhard, M.H., Liu, J., and Li, G.S. (2014). Electrochemically stable cathode current collectors for rechargeable magnesium batteries. *J. Mater. Chem. A* **2**, 2473–2477.
  - Liao, C., Sa, N., Key, B., Burrell, A.K., Cheng, L., Curtiss, L.A., Vaughey, J.T., Woo, J.-J., Hu, L., Pan, B., and Zhang, Z. (2015). The unexpected discovery of the  $\text{Mg}(\text{HMDS})_2/\text{MgCl}_2$  complex as a magnesium electrolyte for rechargeable magnesium batteries. *J. Mater. Chem. A* **3**, 6082–6087.
  - Yu, X., and Manthiram, A. (2017). Electrochemical energy storage with mediator-ion solid electrolytes. *Joule* **1**, 453–462.
  - Lin, M.-C., Gong, M., Lu, B., Wu, Y., Wang, D.-Y., Guan, M., Angell, M., Chen, C., Yang, J., Hwang, B.-J., and Dai, H. (2015). An ultrafast rechargeable aluminium-ion battery. *Nature* **520**, 324–328.

43. Wang, F., Borodin, O., Gao, T., Fan, X., Sun, W., Han, F., Faraone, A., Dura, J.A., Xu, K., and Wang, C. (2018). Highly reversible zinc metal anode for aqueous batteries. *Nat. Mater.* *17*, 543–549.
44. Dong, H., Li, Y., Liang, Y., Li, G., Sun, C.-J., Ren, Y., Lu, Y., and Yao, Y. (2016). A magnesium-sodium hybrid battery with high operating voltage. *Chem. Commun. (Camb.)* *52*, 8263–8266.
45. Strauss, S.H. (1993). The search for larger and more weakly coordinating anions. *Chem. Rev.* *93*, 927–942.
46. Yoo, H.D., Liang, Y.L., Li, Y.F., and Yao, Y. (2015). High areal capacity hybrid magnesium-lithium-ion battery with 99.9% coulombic efficiency for large-scale energy storage. *ACS Appl. Mater. Interfaces* *7*, 7001–7007.
47. Cheng, Y.W., Chang, H.J., Dong, H., Choi, D., Sprenkle, V.L., Liu, J., Yao, Y., and Li, G.S. (2016). Rechargeable Mg-Li hybrid batteries: status and challenges. *J. Mater. Res.* *31*, 3125–3141.
48. Kraychyk, K.V., Wang, S., Piveteau, L., and Kovalenko, M.V. (2017). Efficient aluminum chloride natural graphite battery. *Chem. Mater.* *29*, 4484–4492.
49. Sa, N.Y., Pan, B.F., Saha-Shah, A., Hubaud, A.A., Vaughey, J.T., Baker, L.A., Liao, C., and Burrell, A.K. (2016). Role of chloride for a simple, non-Grignard Mg electrolyte in ether-based solvents. *ACS Appl. Mater. Interfaces* *8*, 16002–16008.
50. Chung, S.-H., Chang, C.-H., and Manthiram, A. (2018). Progress on the critical parameters for lithium-sulfur batteries to be practically viable. *Adv. Funct. Mater.* *28*, 1801188.

**JOUL, Volume 3**

**Supplemental Information**

**Directing Mg-Storage Chemistry  
in Organic Polymers  
toward High-Energy Mg Batteries**

**Hui Dong, Yanliang Liang, Oscar Tutusaus, Rana Mohtadi, Ye Zhang, Fang Hao, and Yan Yao**

## **Supplemental Experimental Procedures**

### **Synthesis of organic electrode materials:**

P(NDI2OD-T2) was obtained from Polyera Corp. as reported.<sup>1</sup> P14AQ was synthesized as reported.<sup>2</sup> DMBQ was purchased from TCI America and used without further purification. Mg(TFSI)<sub>2</sub> was dried under vacuum for 24 h at 250 °C. Solvents were pretreated with molecular sieves (Aldrich, 3 Å beads, 4-8 mesh) for two days before use unless otherwise specified.

### **Preparation of 0.25 M Mg(TFSI)<sub>2</sub> and 0.5 M MgCl<sub>2</sub> in DME electrolyte:**

The electrolyte synthesis was carried out inside an Ar-filled glove box (M-Braun). In a typical synthesis of 5 ml 0.25 M Mg(TFSI)<sub>2</sub> and 0.5 M MgCl<sub>2</sub> electrolyte, 0.73 g Mg(TFSI)<sub>2</sub> powder (Solvionic, 99.5%) was added to a suspension of MgCl<sub>2</sub> (Alfa Aesar, 99.999%, 0.24 g in 5 ml DME) in a 10 ml glass vial. The mixture was stirred at 70 °C for 6 h in a sand bath and then cooled down to room temperature to afford a clear solution.

### **Preparation of 0.2 M Mg(TFSI)<sub>2</sub> in diglyme electrolyte:**

In a typical synthesis of 5 ml 0.2 M Mg(TFSI)<sub>2</sub> electrolyte, 0.58 g Mg(TFSI)<sub>2</sub> powder (Solvionic, 99.5%) was added to 5 ml diglyme in a 10 ml glass vial under stirring at room temperature for 2 h to afford a clear solution.

### **Preparation of 0.3 M Mg(HMDS)<sub>2</sub> and 1.2 M MgCl<sub>2</sub> in THF electrolyte:**

In a typical synthesis of 5 ml 0.3 M Mg(HMDS)<sub>2</sub> and 1.2 M MgCl<sub>2</sub> electrolyte, 0.52 g Mg(HMDS)<sub>2</sub> powder (Sigma-Aldrich, 97%) was added to a suspension of MgCl<sub>2</sub> (Alfa

Aesar, 99.999%, 0.57 g in 5 ml THF) in a 10 ml glass vial. The mixture was stirred at room temperature for 48 h to afford a clear solution.

**Preparation of 0.3 M Mg(CB<sub>11</sub>H<sub>12</sub>)<sub>2</sub> in tetraglyme and 0.5 mol kg<sup>-1</sup> Mg(CB<sub>11</sub>H<sub>12</sub>)<sub>2</sub> in DOL/DME (1:1, w/w) electrolytes:**

[Mg(DME)<sub>3</sub>](CB<sub>11</sub>H<sub>12</sub>)<sub>2</sub> was synthesized as reported.<sup>3</sup> In a typical synthesis of 0.3 M Mg(CB<sub>11</sub>H<sub>12</sub>)<sub>2</sub> in tetraglyme, [Mg(DME)<sub>3</sub>](CB<sub>11</sub>H<sub>12</sub>)<sub>2</sub> (279.7 mg) was dissolved in anhydrous tetraglyme (1.542 ml, dried as reported<sup>4</sup>) with stirring and the resulting clear solution was vigorously stirred under vacuum for 15 mins to remove DME solvent. In a typical synthesis of 1.5 ml 0.5 mol kg<sup>-1</sup> Mg(CB<sub>11</sub>H<sub>12</sub>)<sub>2</sub> in DOL/DME (1:1, w/w), [Mg(DME)<sub>3</sub>](CB<sub>11</sub>H<sub>12</sub>)<sub>2</sub> (379.5 mg) was added to 542.5 mg of DME and 717.8 mg of DOL and stirred at room temperature to afford a clear solution.

**Characterizations:**

The electrodes at different discharge and charge states were characterized by XPS (Physical Electronics Model 5700), ICP-OES (Agilent Technologies, Model 725), and EDS. Energy-dispersive X-ray (EDX) spectroscopy measurement was conducted using a JEOL JSM 6400 SEM and an EDAX with Octane Silicon Drift Detector (SDD). The electrodes were taken out from disassembled cells in an Ar-filled glove box. The electrodes were dipped in anhydrous DME or THF for 3 min, and this procedure was repeated 3 times. The washed electrodes were then vacuum-dried at room temperature for 2 h before characterizations.

**Table S1. Performance parameters of cells based on MgCl<sub>2</sub>-storage chemistry.**

Cathode	Electrolyte	Temperature	C <sub>c</sub> (mAh g <sup>-1</sup> )	C <sub>a</sub> (mAh g <sup>-1</sup> )	c (wt%)	C <sub>e</sub> (mAh g <sup>-1</sup> )	E (V)	Specific energy (Wh kg <sup>-1</sup> )
DMBQ	MgCl <sub>2</sub> - Mg(TFSI) <sub>2</sub> in DME	RT	225	2205	4.5	25.3	1.63	36
P14AQ	MgCl <sub>2</sub> - Mg(HMDS) <sub>2</sub> in THF	RT	146	2205	10.3	58.1	1.30	53

C<sub>c</sub> is cathode specific capacity; C<sub>a</sub> is anode specific capacity; C<sub>e</sub> is the apparent specific capacity of the electrolyte; c is weight percentage of the solute (MgCl<sub>2</sub>) in the electrolyte; E is the average discharge voltage.

**Table S2. Performance parameters cells based on Mg-storage chemistry.**

Cathode	Electrolyte	Temperature (°C)	C <sub>c</sub> (mAh g <sup>-1</sup> )	C <sub>a</sub> (mAh g <sup>-1</sup> )	E (V)	Specific energy (Wh kg <sup>-1</sup> )
Mo <sub>6</sub> S <sub>8</sub>	(tert-BuOMgCl) <sub>6</sub> -AlCl <sub>3</sub> in THF	RT	100	2205	1.10	105
		50	129	2205	1.15	140
c-Ti <sub>2</sub> S <sub>4</sub>	PhMgCl-AlCl <sub>3</sub> in THF	RT	130	2205	1.00	123
		60	192	2205	1.20	212
P(NDI2OD-T2)	Mg(TFSI) <sub>2</sub> in diglyme	RT	54	2205	1.44	76
P14AQ	Mg(TFSI) <sub>2</sub> in diglyme	RT	193	2205	1.37	243

C<sub>c</sub> is cathode specific capacity; C<sub>a</sub> is anode specific capacity; E is the average discharge voltage.

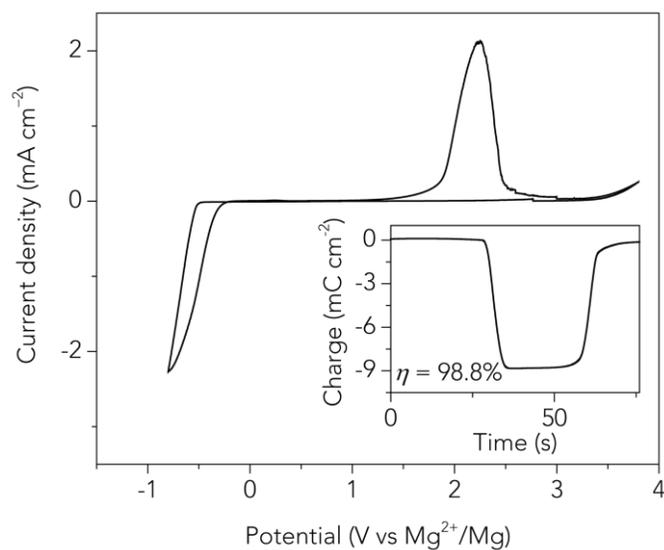


**Figure S1. Cyclic Voltammogram (5<sup>th</sup> cycle) for Mg Metal Plating/Stripping in 0.2 M Mg(TFSI)<sub>2</sub> in Diglyme.**

The working electrode is platinum wire, and both counter and reference electrodes are magnesium ribbons. Inset: Cumulative charge over time. Scan rate: 100 mV s<sup>-1</sup>.

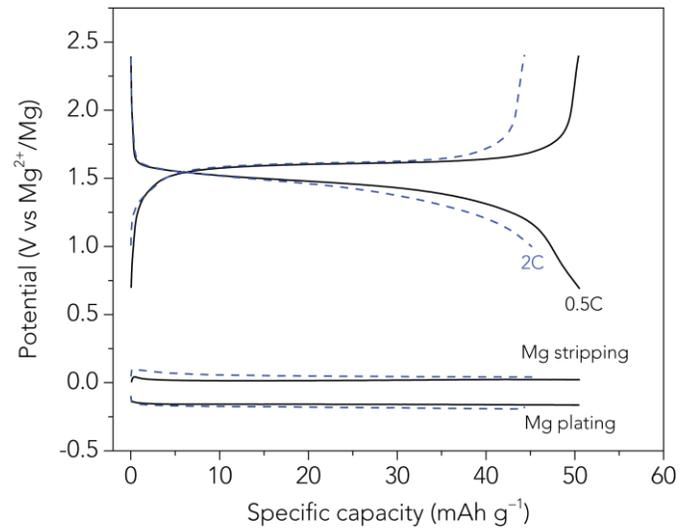


**Figure S2.** The voltage profiles of P(NDI2OD-T2) and Mg in 0.3 M Mg(CB<sub>11</sub>H<sub>12</sub>)<sub>2</sub> in tetraglyme. The charge–discharge rates 0.5 and 2C correspond to current densities of 0.027 and 0.108 mA cm<sup>-2</sup>, respectively.

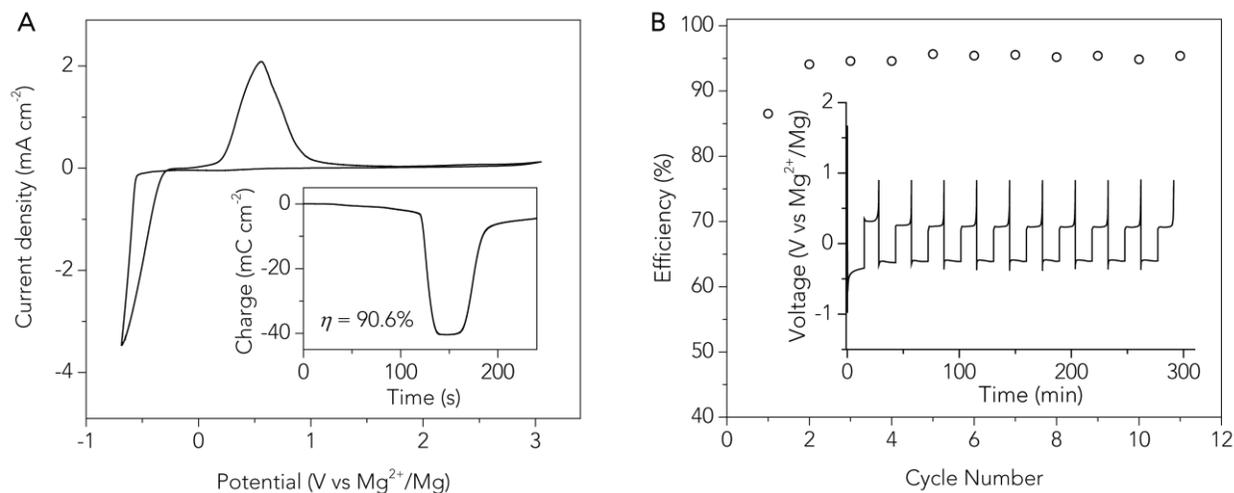


**Figure S3. Electrochemical Performance of  $0.5 \text{ mol kg}^{-1} \text{ Mg}(\text{CB}_{11}\text{H}_{12})_2$  in DOL-DME.**

(A) CV (1<sup>st</sup> cycle) for Mg Metal Plating/Stripping in  $0.5 \text{ mol kg}^{-1} \text{ Mg}(\text{CB}_{11}\text{H}_{12})_2$  in

DOL-DME. The working electrode is platinum wire, and both counter and reference electrodes are magnesium ribbons. Scan rate:  $25 \text{ mV s}^{-1}$ .

(B) Coulombic efficiency of an asymmetric cell for Mg deposition on copper foil versus an Mg negative electrode. The inset is the voltage profiles of Mg deposition/stripping.

Current density:  $0.5 \text{ mA cm}^{-2}$ .

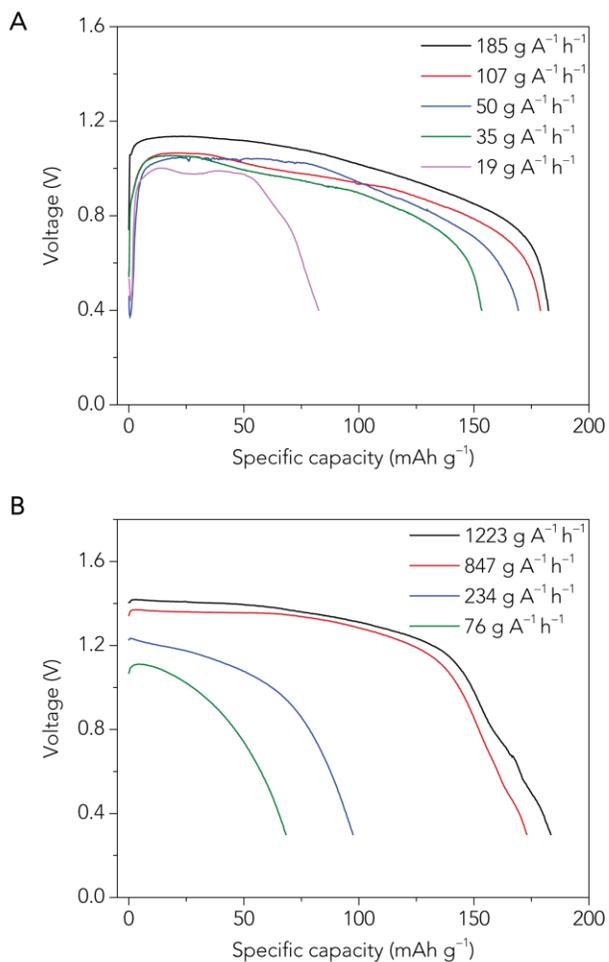


**Figure S4. The Discharge Voltage Profiles of P14AQ with Different Electrolyte/Capacity Ratios.**

(A) Mg<sup>2+</sup> storage at a current of 0.2 C (1C = 260 mA g<sup>-1</sup>) in 0.5 mol kg<sup>-1</sup> Mg(CB<sub>11</sub>H<sub>12</sub>)<sub>2</sub> in DOL–DME.

(B) MgCl<sup>+</sup> storage at a current of 0.2C (1C = 260 mA g<sup>-1</sup>) in 1.2 M MgCl<sub>2</sub> and 0.3 M Mg(HMDS)<sub>2</sub> in THF.

## References:

1. Chen, Z.H., Zheng, Y., Yan, H., and Facchetti, A. (2009). Naphthalenedicarboximide- vs perylenedicarboximide-based copolymers. synthesis and semiconducting properties in bottom-gate n-channel organic transistors. *J. Am. Chem. Soc.* *131*, 8-9.
2. Pan, B.F., Huang, J.H., Feng, Z.X., Zeng, L., He, M.N., Zhang, L., Vaughey, J.T., Bedzyk, M.J., Fenter, P., Zhang, Z.C., Burrell, A.K., and Liao, C. (2016). Polyanthraquinone-based organic cathode for high-performance rechargeable magnesium-ion batteries. *Adv. Energy Mater.* *6*, 1600140.
3. Singh, N., Arthur, T.S., Tutusaus, O., Li, J., Kisslinger, K., Xin, H.L., Stach, E.A., Fan, X., and Mohtadi, R. (2018). Achieving high cycling rates via in situ generation of active nanocomposite metal anodes. *ACS Appl. Energy Mater.* *1*, 4651-4661.
4. Tutusaus, O., Mohtadi, R., Arthur, T.S., Mizuno, F., Nelson, E.G., and Sevryugina, Y.V. (2015). An efficient halogen-free electrolyte for use in rechargeable magnesium batteries. *Angew. Chem. Int. Ed.* *54*, 7900-7904.